Atmos. Chem. Phys. Discuss., 14, 8095–8142, 2014
www.atmos-chem-phys-discuss.net/14/8095/2014/
doi:10.5194/acpd-14-8095-2014

Atmospheric Chemistry and Physics Discussions
Open Access

On the submicron aerosol distributions and CCN number concentrations in and around the Korean Peninsula

J. H. Kim[1], S. S. Yum[1], S. Shim[1], W. J. Kim[1], M. Park[1], J. Kim[2], M. Kim[2], and S. C. Yoon[2]

[1]Department of Atmospheric Sciences, Yonsei University, Seoul, Korea
[2]School of Earth and Environmental Sciences, Seoul National University, Seoul, Korea

Received: 27 January 2014 – Accepted: 6 March 2014 – Published: 25 March 2014

Correspondence to: S. S. Yum (ssyum@yonsei.ac.kr)

Published by Copernicus Publications on behalf of the European Geosciences Union.

On the submicron aerosol distributions and CCN number concentrations

J. H. Kim et al.

Abstract

Total number concentrations of particles having diameter larger than 10 nm (N_{CN}), cloud condensation nuclei at several supersaturation (S) values (N_{CCN}), and the number size distribution of particles for 10–414 nm particle diameter range were measured in Seoul between 2004 and 2010. Overall average values of N_{CN} and geometric mean diameter are 17 811 ± 5581 cm^{-3} and 48 ± 6 nm, respectively. Average N_{CCN} at 0.4, 0.6, and 0.8 % S are 4145 ± 2016, 5323 ± 2453 and 6067 ± 2780 cm^{-3}, respectively and corresponding N_{CCN}/N_{CN} are 0.26 ± 0.11, 0.33 ± 0.11 and 0.37 ± 0.12. There is a clear seasonal variation of aerosol concentration, which seems to be due to the monsoon. N_{CN} and N_{CCN} are also found to be dependent on the volume of traffic and the height of planetary boundary layer, respectively.

During the two aircraft campaigns in 2009 and 2011, N_{CN} and N_{CCN} at 0.6 % S were measured in and around the Korean Peninsula. During the 2011 campaign, aerosol scattering coefficient was also measured. N_{CN} and N_{CCN}0.6 in the lower altitudes were generally higher than at higher altitudes, except for the cases when particle formation and growth events are thought to occur at higher altitudes. N_{CN} and N_{CCN}0.6 show generally a positive correlation with aerosol scattering coefficients but its correspondence tends to vary with altitude. Occasional instances of low (< 0.3) $N_{CCN}0.6/N_{CN}$ in the boundary layer are demonstrated to be associated with particle formation and growth events. With the support of ground measurements, it is confirmed that a particle formation and growth event indeed occurred on a flight day over the Yellow Sea and the areal extent of the event is estimated to be greater than 100 km × 450 km.

With the combination of the current and several relevant previous studies, a composite map of N_{CN} and N_{CCN} in and around the Korean Peninsula is produced. Overall, the exhibited concentrations are typical of the values measured over the polluted regions elsewhere in the globe. Moreover, there is a generally decreasing trend from west to east over the region, implying that the region is constantly under the dominant influence of continental outflow.

ACPD
14, 8095–8142, 2014

1 Introduction

With increasing attention on climate change in general, interest in cloud condensation nuclei (CCN) due to its effects on various cloud properties including cloud albedo and lifetime (i.e., aerosol indirect effects) is not limited within the cloud physics community but wide spread throughout the atmospheric science, climate science and aerosol science communities. With an increasing fear that societies as a whole are not adopting the necessary measures required to prevent catastrophic climate change quickly enough (Rojeli et al., 2011), it also sparked a debate on so-called "geo-engineering" (Crutzen, 2006; Robock, 2008).

The aerosol indirect effects on climate have attracted many researchers not only because its magnitude is estimated to be large enough to compensate a significant portion of the greenhouse gas effect but also because its uncertainty is large (IPCC, 2007), especially when it comes to determining the climate sensitivity (Kiehl, 2007; Schwartz et al., 2010). One of the several reasons behind such large uncertainty is that aerosol properties exhibit high geographical heterogeneity due to its short lifetime in the atmosphere (∼ days) compared to greenhouse gases (∼ years) (IPCC, 2007). Such heterogeneity makes it difficult for scientists to draw a global and long term picture of aerosol contributions. Therefore securing aerosol dataset of global coverage is important, especially that of the number concentration, which is of primary concern when it comes to cloud and aerosol interaction problem because the number of cloud droplets is initially determined by the number of aerosol particles that can be activated as embryonic cloud droplets at a given supersaturation (S). Such information is relatively scarce in East Asia compared to those in Europe and North America (Kumala et al., 2004), although various efforts have been put forth in recent years, including the ones that tried to characterize the new particle formation (Weber et al., 2003; Buzorius et al., 2004; McNaughton et al., 2004; Wu et al., 2007; Lee et al., 2008; Park et al., 2008; Wiedensohler et al., 2009; Song et al., 2010; J. H. Kim et al., 2012, Y. Kim et al., 2013) and CCN properties (Matsumoto et al., 1997; Adhikari et al., 2005; Yum et al.,

ACPD
14, 8095–8142, 2014

2005, 2007; J. H. Kim et al., 2011; Kuwata and Kondo, 2008; Kuwata et al., 2008; Mochida et al., 2010; Rose et al., 2010).

This study is an addition to this effort and aims at characterizing the number concentration of submicron aerosols (i.e., condensation nuclei, CN) (N_{CN}) and CCN (N_{CCN}) measured in and around the Korean Peninsula, which is strategically located about 500 km downwind of the Chinese continent (considering the prevailing westerly winds in this region) and therefore suitable for monitoring the continental outflow at first hand.

This study first focuses on the aerosol and CCN characteristics measured in Seoul that may represent a typical large urban city in East Asia. About 1000 and 800 days, respectively, of CN and CCN data, which cover the years between 2004 and 2010, are analyzed in order to provide statistically robust result. It is suggested that while the majority of CN observed in Seoul had local origin, the same could not be said for CCN.

Then we present the CN and CCN data observed during two aircraft measurement campaigns in and around the Korean Peninsula. Up to our knowledge, these are the first attempts to illustrate such data over the Korean Peninsula. The main purpose of these campaigns was to verify from in-situ measurements if there really was the east-west gradient of aerosol concentrations in the continental outflow region as exemplified by Y.-J. Kim et al. (2011) that showed the smoothly decreasing trend of aerosol optical depth (AOD) from China to the East Sea by averaging the satellite retrieved AOD data for several years. The vertical profiles of N_{CN} and N_{CCN} measured during the two campaigns varied a lot but the concentrations were generally higher in the planetary boundary layer (PBL) than over the free troposphere and the concentrations in the PBL were higher over the Yellow Sea than over the East Sea, indeed demonstrating the east-west gradient.

Lastly, we provide the composite map of N_{CN} and N_{CCN} in the PBL in and around the Korean Peninsula by combining the data presented in this study with those from several previous measurement studies at various platforms in this region: rural sites (Yum et al., 2005; Kim et al., 2012), island sites (Yum et al., 2007; J. H. Kim et al., 2011) and cruise ships (Kim et al., 2009). Statistically robust results from Seoul enabled us to

ACPD
14, 8095–8142, 2014

distinguish the characteristics that may be shared with other regions within the Korean Peninsula from the ones arising from local sources in Seoul. Aircraft measurements provided us the data at the locations where ground measurements could not cover such as the Yellow Sea and the East Sea. This map is the product of 8 years long effort to measure the aerosol size distribution and CCN concentration in the PBL over this region (all but one study used the very same instruments). Considering the fact that aerosol concentrations, especially N_{CCN}, did not vary much within the PBL as shown in this study, these concentrations should be highly relevant to the cloud droplet concentrations of the clouds whose base is within the PBL. Therefore this composite map is highly expected to be used as a valuable reference dataset for modeling studies and for satellite remote sensing retrieval of the aerosol distribution in East Asia.

2 Seoul measurement (2004–2010)

Seoul (37.6° N, 127.0° E) is a megacity of which the population is more than 10 million. Owing to numerous anthropogenic sources and large seasonal variation due to monsoon, Seoul's aerosol properties cannot be characterized from a few intensive campaigns. Here we present a long term measurement data for the period from 2004 to 2010.

2.1 Method

N_{CN} and submicron aerosol size distribution data were measured at the Yonsei University campus located at the northwestern part of Seoul by TSI CPC3010 and SMPS 3936L10, respectively. The instruments were placed at a 6th floor room of a building in the campus which is about 300 m away from the major traffic road outside the campus and therefore were safely removed from the immediate influence of traffic emissions in the campus and in the major road. The data were obtained every 1 and 180 s for CN and aerosol size distribution, respectively, and accumulated since June and September 2004, respectively, until the end of December 2010. Due to very high N_{CN} in Seoul, the sample air for N_{CN} was diluted by splitting the sample flow into two branches and passing one of them through HEPA filter to remove all the particles in the air that went through it and then combining it with the other branch before feeding it into the instrument. The flow of each branch was measured every one or two weeks and the resulting dilution factor was mostly between 2.5 and 3.0. N_{CCN} measurement started at the same site since September 2006 with the single column CCN counter (CCNC) from Droplet Measurement Technologies. The instrument produced the data every 1 s and was calibrated with the method identical to the one illustrated in J. H. Kim et al. (2011).

Because the instruments had to be deployed for various field campaigns (e.g. Yum et al., 2005, 2007; Kim et al., 2009; J. H. Kim et al., 2011, 2012) total of 981, 1066, 797 days of data were collected for N_{CN}, aerosol size distribution and N_{CCN}, respectively, which covers about 41–50 % of the days in the corresponding period. There are more aerosol size distribution data than N_{CN} data due to the optics contamination issue for CPC arising from the high level of air pollution in Seoul.

Average N_{CN} value is obtained by averaging the total of 53 monthly averaged values, each of which is again the average of about 19 daily averaged values. Average D_g is obtained in the similar fashion, with the total of 52 months and about 20 days for each month. Average N_{CCN} at 0.4, 0.6 and 0.8 % S is from 35 monthly averaged values (about 23 days for each month) and N_{CCN}/N_{CN} is from the 28 months (about 22 days each) when N_{CCN} and N_{CN} were simultaneously available.

2.2 Results

2.2.1 Overall statistics

Figure 1 shows the temporal variation of the monthly average values of N_{CN}, N_{CCN}, geometric mean diameter (D_g) and N_{CCN}/N_{CN}. A seasonal variation is obvious as will be discussed in detail below. The average submicron aerosol size distribution for the whole period is shown in Fig. 2. The average values of N_{CN} and D_g are 17 811 ± 5581 cm^{-3}

ACPD
14, 8095–8142, 2014

and 48 ± 6 nm, respectively. The average N_{CCN} at 0.4, 0.6, and 0.8 % S (N_{CCN}0.4, N_{CCN}0.6, and N_{CCN}0.8) are 4145 ± 2016, 5323 ± 2453 and 6067 ± 2780 cm^{-3}, respectively. The corresponding ratio of N_{CCN}/N_{CN} are 0.26±0.11, 0.33±0.11 and 0.37±0.12, respectively.

N_{CN} measured in Seoul is much lower than the one measured in some other megacities of Asia such as New Delhi, India (Mönkkönen et al., 2005) or Beijing, China (Wu et al., 2007). It is comparable to the one measured in Guangzhou, China (Rose et al., 2010) and is much higher than the one measured in Tokyo, Japan (Kuwata and Kondo, 2008). Compared to rural sites in Europe, it is higher at least by a factor of two (Asmi et al., 2011). N_{CCN} is much lower than the ones measured in Beijing (Weidensohler et al., 2009) and Guangzhou, but higher than that measured in Tokyo.

Figure 3 is the scatterplot of simultaneously measured, hourly averaged D_g vs. $N_{CCN}0.6/N_{CN}$ that shows a strongly positive correlation. Interpreting $N_{CCN}0.6/N_{CN}$ as an average probability of a randomly selected particle acting as CCN (for a few data in Fig. 3 the value exceeds one due to instrumental differences between TSI CPC 3010 and DMT CCNC), and D_g as its average diameter, it can be said that the sizes of the particles determined the CCN activity to a certain degree. However, it should also be pointed out that $N_{CCN}0.6/N_{CN}$ values vary quiet significantly for a constant D_g in Fig. 3, especially for the diameter range between 40 and 70 nm. It implies that while the size may have been the primary factor for determining whether a particle would act as CCN or not, there were still some other factors (e.g. chemical composition) that affected the CCN activity of particles in Seoul.

2.2.2 Seasonal variation

Monthly average values of N_{CN}, N_{CCN}0.4, N_{CCN}0.6, N_{CCN}0.8, N_{CCN}/N_{CN} and D_g are shown in Fig. 4b and c. The values are first daily averaged and then averaged for the month of the year. Number of monthly measurement days for each instrument is also shown in Fig. 4a. N_{CN} and N_{CCN} during the winter (December–February) are

Discussion Paper | Discussion Paper | Discussion Paper | Discussion Paper |
ACPD
14, 8095–8142, 2014

about twice higher than those during the summer (June–July). It may be suspected that the wintertime heating emission might have contributed to the high concentrations in winter. However, N_{CN} and N_{CCN} are not particularly higher on colder days when more heating was expected (not shown). The seasonal variation of N_{CN} and N_{CCN} can be attributed to the monsoon that generally brings continental air during the winter and the maritime air from the Pacific during the summer to the Korean Peninsula. Monsoon also brings more than half of the annual precipitation during the summer in Seoul. However, negligible correlation is found between N_{CCN} or N_{CN}, and the daily precipitation amount for the summer months. It reduces the possibility that the low concentrations during the summer months are solely due to precipitation scavenging. Even on the record breaking day of 259 mm precipitation (21 September 2010), N_{CN} and $N_{CCN}0.6$ are close to 70 % of the average values of that month and there were other days in that month exhibiting even lower concentrations.

In Fig. 4c, D_g is the largest in March and April when Asian Dust events occur the most frequently (Kim, 2008), which implies that the sizes of submicron particles in Seoul were being affected by these events. The largest D_g, however, does not result in the highest N_{CCN}/N_{CN} for these two months as would be expected from Fig. 3. It means that the particle sizes were the largest but their hygroscopicity was very low in these two months, explaining the large vertical spread of N_{CCN}/N_{CN} for a constant D_g value in Fig. 3. For each CCN spectrum obtained every 30 min, the parameter k for the power law relationship ($N_{CCN} = C \times S^k$) known as the "Twomey equation" was calculated and its monthly averaged values are shown in Fig. 4c. Parameter k is the slope of the CCN spectrum in log-log plot (for 0.4–0.8 % S range) and indicates how fast N_{CCN} increases with S. If the chemical composition is the same for all particles, k will be higher when the portion of smaller particles that can be activated as cloud droplets at higher S is larger and vice versa. Therefore it is understandable that k seems to have a negative relationship with D_g in Fig. 4c. However, k is the highest in December when D_g is not particularly small compared to the other months. Such high k can be explained if relatively large portion of the particles measured in December required

ACPD
14, 8095–8142, 2014

high S to be activated as cloud droplets even though the sizes were not small, implying relatively low aerosol hygroscopicity in December. Nevertheless, these particles were considered to be more hygroscopic than the particles measured in March and April: see the low N_{CCN}/N_{CN} in these two months despite the large D_g.

2.2.3 Diurnal variation

Diurnal variations were obtained by averaging the data every 30 min (N_{CN}, N_{CCN} and D_g) or every one hour (N_{CCN}/N_{CN} and k) bin for the day. The average number of the data used to represent each time bin are 897 ± 7, 725 ± 9, 715 ± 9, 695 ± 19 and 967 ± 7 for N_{CN}, $N_{CCN}0.4$, $N_{CCN}0.6$, $N_{CCN}0.8$ and D_g, respectively. Similarly the numbers are 552±5, 552±6, 549±7 and 729±7 for $N_{CCN}0.4/N_{CN}$, $N_{CCN}0.6/N_{CN}$, $N_{CCN}0.8/N_{CN}$ and k, respectively. Seasonally classified diurnal variations are shown in Fig. 5. There is a clear minimum before the dawn and the mid-morning and evening peaks for N_{CN}. This diurnal pattern changes little from season to season except that the concentration itself is much higher during winter than the other seasons (Fig. 5a). N_{CCN} show a different pattern from N_{CN}: early morning minimum is not very conspicuous or never exists and the mid-morning maximum is pronounced only in winter (Fig. 5b). Now we examine the possible reasons for these diurnal patterns.

Traffic amount

The average diurnal variations of N_{CN}, $N_{CCN}0.6$, $N_{CCN}0.6/N_{CN}$, D_g and k for the entire period are shown in Fig. 6 along with the hourly averaged traffic amounts on the major road just outside the Yonsei University campus (∼ 300 m from the measurement site). Traffic data are limited only for 25 days mostly during autumn but the traffic trend is expected not to differ significantly for different seasons. It is reported that in Seoul 30 % and 70 % of the vehicles on the road use diesel and gasoline as their fuel, respectively (Pandey et al., 2008).

The most prominent feature in Fig. 6 is that the time of the minimum N_{CN} around 4–5 a.m. coincides with that of the traffic amount. The time of the maximum N_{CN} at 7–8 p.m. slightly lags that of the traffic amount (6–7 p.m.). N_{CN} increases sharply during 5–8 a.m., which is in accordance with the increasing traffic amount in these hours. Strikingly similar behavior for nitric oxide (NO) concentration was reported (Pandey et al., 2008). Such similarity suggests that the traffic, which is a primary source of NO, is also the main contributor of N_{CN} in Seoul. Such similarity seems not obvious for N_{CCN}, implying that traffic emission may not have been the primary source of N_{CCN}. However, N_{CCN} is not completely independent from the traffic emission. Figure 7 shows the relationship between the hourly-averaged values of traffic amount and N_{CCN} or N_{CN}. If we interpret N_{CN} as N_{CCN} at a very high S (i.e., $> 0.8\,\%$), we can say that the correlation becomes more significant with increasing S. It implies then that the particles originated from traffic emission were more likely to be the particles that could be activated mostly at higher S, probably because they were smaller and less hygroscopic.

Planetary boundary layer height

Planetary boundary layer (PBL) height can have an effect on N_{CN} and N_{CCN} because the atmosphere becomes diluted as PBL expands. Due to the lack of the atmospheric thermodynamic sounding data with sufficiently high temporal resolution, we analyzed instead the Continuous Micro Pulse Lidar (MPL) measurement data obtained at the Seoul National University campus in Seoul (Kim et al., 2007) to estimate the PBL height. Seoul National University is located 11 km south of our measurement site. MPL measures the vertical profile of aerosol attenuated backscatter coefficient at 532 nm wavelength every 15 min. Automated wavelet covariance transform (WCT) method from Brooks (2003) was applied to the backscatter profiles obtained from August 2006 to December 2010. Only the days when there was no precipitation and the daily cloud amount was less than 1/10 were selected and 213 days (mostly during winter) met those criteria during the above period.

ACPD
14, 8095–8142, 2014

For the selected days, the average diurnal variation of PBL height shows almost no seasonal variation although the maximum PBL height of the day differs from season to season: about 1500 m during summer and lower than 1000 m during winter (not shown). Generally it starts to rise around 9 a.m., reaches the maximum at about 4 p.m., reduces to the height of 600–800 m at about midnight and stays largely at this value throughout the night. When this night period is excluded there is a remarkably consistent but opposite trend between the PBL height and $N_{CCN}0.6$ as shown in Fig. 8, where the normalized PBL height and $N_{CCN}0.6$ are shown together with the axis for the normalized PBL height reversed. The normalization is done for each day by converting the daily maximum and minimum values of $N_{CCN}0.6$ to 1.0 and 0.0, respectively. Normalized PBL height is similarly obtained. In this way the influence of daily fluctuation is removed for both parameters. However, the days when both parameters were simultaneously measured almost throughout a day (more than 18 h) were limited (40 days) and they were usually not consecutive. Along with the normalization process itself, this is the main reason why the values just before and after midnight are not smoothly varied especially for normalized $N_{CCN}0.6$ in Fig. 8.

Figure 9 shows the scatterplot of the hourly-averaged PBL height vs. N_{CCN} and N_{CN} in a manner similar to Fig. 7. Note that N_{CN} and N_{CCN} in Fig. 9 are higher than the corresponding values in Fig. 7 because in Fig. 9 the data mostly from winter are used to calculate N_{CN} and N_{CCN} to match the time of MPL data while the data used in Fig. 7 are mostly from autumn as mentioned in the previous section. The data points for 09:00–24:00 LT are highlighted with circle in Fig. 9 and as expected from Fig. 8 N_{CCN} for all S show strong negative correlations with the PBL height. However, no such tendency is found for N_{CN}. These contrasting results seem to be related to the diurnal variation of traffic amount and its much closer relationship with N_{CN} than with N_{CCN}. For N_{CN} the increased traffic amount that reaches nearly its daily maximum at 9 a.m. can compensate the dilution effect of PBL height which starts to expand at this hour (Fig. 8). After 4 p.m., the PBL height starts to shrink but the traffic amount starts to decrease as well a few hours later (6 p.m.) and therefore the concentrating effect of

Discussion Paper | Discussion Paper | Discussion Paper | Discussion Paper |

ACPD
14, 8095–8142, 2014

On the submicron aerosol distributions and CCN number concentrations

J. H. Kim et al.

descending PBL height is again compensated by decreasing traffic amount. Because traffic emission has only a secondary importance for N_{CCN}, such compensations do not seem to occur and the effect of dilution and concentration due to PBL height variation is fully exerted for N_{CCN}. From midnight to 9 a.m., PBL height shows little variation and therefore the traffic emission seems to act as the single most important factor driving both N_{CN} and N_{CCN}.

3 Airborne measurement (2009, 2011)

3.1 Instrumentation

Two aircraft campaigns were conducted using a Beechcraft King Air (C90GT) aircraft. The first one was conducted during 30 September–18 October 2009 and the second one during 8–17 June 2011. For both campaigns DMT CCNC and TSI CPC 3010 were used to measure N_{CCN} and N_{CN}, respectively. For the 2011 campaign, TSI Nephelometer 3536 was also onboard the aircraft and measured scattering coefficients at three wavelengths – 450, 500 and 700 nm. All the instruments were calibrated before each campaign. Because the internal S field within the CCNC varies with ambient pressure (Robert and Nenes, 2005), CCNC was operated with the fixed internal S of 0.6 % and the fixed internal pressure of 650 and 530 mb for the 2009 and 2011 campaigns, respectively. Such pressure values were selected to guarantee that they were sufficiently lower than the ambient pressures at the maximum flight altitudes of the two campaigns (3000 m for 2009 and 5000 m for 2011), in order to make it possible to offset the ambient pressure fluctuation with an orifice, an adjustable valve and a pump. The counting efficiency of CPC is known to be insensitive to ambient pressure fluctuation under such pressure range (Zhang and Liu, 1991). The nephelometer was considered not to suffer from ambient pressure fluctuation as well (Bodhaine et al., 1991).

During the 2009 campaign, an isokinetic inlet system was not available and the aircraft cabin window was slightly open to stick out a quarter inch tube and draw the sam-

Discussion Paper | Discussion Paper | Discussion Paper | Discussion Paper |

ACPD

14, 8095–8142, 2014

On the submicron aerosol distributions and CCN number concentrations

J. H. Kim et al.

ple air from outside the aircraft. In order to see the effect of such an an-isokinetic inlet design, additional TSI CPC 3010 was installed on Korea Global Atmosphere Watch Center (KGAWC, 36.5° N, 126.3° E) which is about 7 km away from Tae-An Airport (36.6° N, 126.3° E) where the aircraft took off and landed. It is found that N_{CN} measured during the take-offs and landings (altitude < 400 m) exhibit values larger than N_{CN} measured at KGAWC by 21–55 %. Such values can be interpreted as a representative error arising from using an an-isokinetic inlet. During the 2011 campaign, an isokinetic inlet system was implemented.

3.2 Flight design

The measurement data were obtained from 8 research flights during the 2009 campaign. The flight design was aimed at verifying east-west gradient of N_{CN} and N_{CCN} as explained in Sect. 1. The aircraft took off at Tae-An Airport located at the western coast of the Korean Peninsula and chose one of the two routes. In the first route, it flew out west to 124.7° E over the Yellow Sea; then headed south following the constant longitude line until it reached 33.4° N; then it flew east to Jeju Island (126.3° E); and headed back to Tae-An Airport. This closed circuit route is denoted as "Yellow Sea route". In some flights, the circuit route in exactly the opposite direction was chosen. The second route was to fly east and across the Korean Peninsula and over the East Sea until it reached 131.15° E, then head straight north to Ulleung Island (37.5° N, 130.9° E) and then return to Tae-An, which is called "East Sea route". The two routes are shown in Fig. 10. During most of the flights the aircraft cruised at the altitude of 3000 m, but it made vertical soundings in each leg, spiraling down to an altitude of about 500 m and back up to the cruising altitude. The horizontal area span during the spiral was smaller than 9 km × 10 km.

During the 2011 campaign, the measurement data were obtained from three research flights. The first and second flights took the Yellow Sea route and the East Sea route, respectively. The last flight covered both the Yellow Sea and the East Sea. The vertical soundings were made in the identical manner to that of the 2009 campaign but their maximum altitude was extended to 5000 m.

3.3 Results

3.3.1 Vertical distribution

In total, 17 and 11 vertical soundings were made during the 2009 and 2011 campaigns, respectively (Table 1). For comparison, the vertical soundings are classified into three regions based on the longitudinal location as shown in Fig. 10 – region I (33–37° N × 124–125.7° E) covers the eastern part of the Yellow Sea, region II (33–37.7° N × 125.7–127° E) covers the western coast of the Korean Peninsula and the region III (36–38° N × 130–132° E) covers the East Sea around Ulleung Island. The regions I and II are distinguished to see if the effects of local sources in the western part of the Korean Peninsula could be separated out from the influence of continental outflow. Total of 4, 5 and 8 soundings were made in regions I, II and III, respectively, during the 2009 campaign, and 4, 3 and 4 during the 2011 campaign (Table 1).

N_{CN} and N_{CCN}0.6

Figure 11 shows the average vertical distributions of $N_{CCN}0.6$, N_{CN} and $N_{CCN}0.6/N_{CN}$ for each region from the two campaigns. First, the data are averaged by 100 m altitude bin for each spiral sounding listed in Table 1. These 100 m altitude bin average values are then averaged for each region. In most of the panels in Fig. 11, N_{CN} are relatively higher at lower altitudes, showing the influence of the surface sources. $N_{CCN}0.6$ also shows a similar trend but with smaller vertical gradient, implying that the influence of the surface sources is less pronounced for CCN. On the other hand, $N_{CCN}0.6/N_{CN}$ does not vary much with altitude and the average for the whole depth of each sounding ranges from 0.57 to 0.78 in Fig. 11. Average N_{CN} are comparable to the ones obtained at locations between the Korean Peninsula and Japan during

ACPD
14, 8095–8142, 2014

ACE-ASIA in 2001 (Clarke and Kapustin, 2010) as marked in Fig. 11. It is also worth noting that when the layer with enhanced particle concentration (such as the noticeable bumps observed around 3000 m altitude in panels e and f) is not considered, N_{CN} and $N_{CCN}0.6$ measured near or above 3000 m altitude were also comparable to the ones measured during ACE-1 in 1995 over the Southern Ocean when the air mass was originated from the Australian continent (Hudson et al., 1998). Based on their measurements of N_{CN} and N_{CCN} at 0.3 % S in a southwestern island of Japan, Adhikari et al. (2005) suggested that N_{CCN}/N_{CN} of 0.5 or higher was a characteristic value for continentally/anthropogenically influenced marine air. Consistently we may assess that our values also mostly represents such air mass in East Asia. However, these values are still about a factor of two larger than those in Seoul (discussed above), suggesting greater CCN capability of aerosol particles over the marine region than in a highly urban city.

For both 2009 and 2011 campaigns but especially more for the 2009 campaign, $N_{CCN}0.6$ and N_{CN} below 1000 m altitude are higher over the regions I and II than over the region III (Fig. 11), surely due to the fact that the regions I and II are closer to China and also locally industrial activities are more active in the western than in other parts of Korea. However, there is no significant difference between regions I and II, only somewhat higher concentrations for region II perhaps due to the addition of local sources. The general westward gradient diminishes at higher altitudes, suggesting that the influence of the surface sources are more likely to be confined within the boundary layer. Much smaller standard deviations of $N_{CCN}0.6/N_{CN}$ over the region III at the lowest altitudes suggests that there are less local sources or particle formation events occurring over this region than over the regions I and II.

The relatively large standard deviations as well as the high N_{CN} shown in several panels (e.g. near the surface in a, b and e; between 2300 m and 4000 m altitudes in d) are suspected to be due to occasional particle formation and growth events that led to elevated N_{CN} at the affected region. More detailed discussion on this is given below.

Relationship with scattering coefficient

Vertical distributions of the 300 m altitude bin averaged scattering coefficient (σ) at three wavelengths (450, 550 and 700 nm) and the Angström exponent (AE) measured during the 2011 campaign are shown in Fig. 12 for each of the regions I, II and III. σ values tends to be higher at the western side of the Korean Peninsula than at the eastern side. The σ for 550 nm (σ_{550}) of 50–110 Mm^{-1} below 1000 m altitude is a factor of two to four smaller than those measured in Seoul (~ 200 Mm^{-1}; Shim et al., 2008) but similar to or larger than those observed over the East Asian seas during the ACE-Asia project (Carrico et al., 2003). In Fig. 12 for all three regions there is an elevated σ layer in between 1000 m and 2500 m altitudes and then it decrease with altitude to reach near the detection limit above 4000 m altitude. This trend is not much consistent with the vertical profiles of N_{CN} and $N_{CCN}0.6$ shown in Fig. 11d–f except the rather similar feature in the region III (compare Figs. 11f and 12c). This demonstrates that the particle number concentration is not the only parameter that determines the scattering properties.

However, some previous measurement studies over the Korean Peninsula (Shim et al., 2008; Kim et al., 2012) and in other parts of the globe (Andreae, 2009; Clarke and Kapustin, 2010) suggest a positive correlation between σ vs. N_{CN} and σ vs. $N_{CCN}0.6$. Figure 13 is the scatterplot of simultaneously measured N_{CN} or $N_{CCN}0.6$ vs. σ_{550} for the entire 2011 campaign and indeed seems to suggest that there is a positive correlation although the scatter is large. To note is that there seems be an altitude dependence of the relationship. σ_{550} tends to be smaller at higher altitudes regardless of N_{CN} and $N_{CCN}0.6$ variations. Throughout the entire campaign, CN and CCN0.6 observed at the highest altitudes (> 4500 m) tend to scatter less light: all 357 data points collected above 4500 m altitude are located below the solid line for CN and CCN0.6, respectively, in Fig. 13. In particular, over the region II, N_{CN} and $N_{CCN}0.6$ increase quite significantly above 4900 m altitude (Fig. 11e), but the correspondence for σ is almost negligible (Fig. 12b). A careful examination of the nephelometer data found no instrumental issue for this case, implying that these CN and CCN0.6 indeed had negligible σ. In relation to this unique feature, it is worth mentioning that at higher altitudes $N_{CCN}0.6/N_{CN}$ tends to decrease with altitude for all three flights during the 2011 campaign (Fig. 11d–f). This may suggest that aerosol particles were smaller at higher altitudes and therefore smaller σ_{550}. However, this cannot completely explain the complicated correspondence between σ_{550} and, N_{CN} or $N_{CCN}0.6$ shown in Fig. 13, which reflects the fact that the relation between the number concentration and scattering coefficient of the particles is mediated by various properties. A detailed *analysis* of the factors that regulate the relationship between N_{CN}, N_{CCN} and σ requires further study in the future.

3.3.2 Horizontal distribution at 3000 m altitude

Horizontal distributions of N_{CN} and $N_{CCN}0.6$ are obtained when the aircraft was cruising at the altitude of about 3000 m in the period between the times of the spiraling vertical soundings. The spatial distribution of $N_{CCN}0.6$ is illustrated in Fig. 14. Overall average values of $N_{CCN}0.6$, N_{CN} and $N_{CCN}0.6/N_{CN}$ were 1207± 915 cm^{-3}, 1870± 1463 cm^{-3} and 0.64± 0.06, respectively. Average values of σ for 450, 550 and 700 nm and AE measured during the 2011 campaign were 57.0±42.7 Mm^{-1}, 42.7±31.9 Mm^{-1}, 28.2±21.1 Mm^{-1} and 1.51±0.30, respectively. Average values for each flight and each campaign are shown in Tables 2 and 3.

Most of N_{CN} and $N_{CCN}0.6$ values in Table 2 are much lower than the values measured within the boundary layer around the Korean Peninsula (Sect. 4.2), indicating that aerosol characteristics in the free troposphere are certainly different from those within the boundary layer. However, some high values are observed on some days (10 October 2009, 11 and 12 June 2011), which are comparable to, or even higher than those measured at the surface sites. N_{CN} and $N_{CCN}0.6$ higher than 7000 cm^{-3} and 5000 cm^{-3}, respectively, are also observed during the flights on 15 October 2009 at the eastern coast of the Korean Peninsula (Fig. 14). Such high values may suggest an elevated pollution layer transported from China or local surface emission reaching at

ACPD
14, 8095–8142, 2014

high altitudes without much dilution. The westward gradient of CCN concentration is apparent only in the flight on 11 October 2009 (Fig. 14), which may indicate that the general westward gradient of aerosol concentrations (Fig. 11) or AOD (Y.-J. Kim et al., 2011) is mostly determined by the aerosols in the lower atmosphere.

4 Discussion

4.1 Particle formation and growth events

Buzorius et al. (2004), Lee et al. (2008) and Kim et al. (2009) all independently reported the particle formation and growth events observed over the Yellow Sea. Yum et al. (2007) and Kim et al. (2013) also reported such events at Gosan, Jeju Island (33.2° N, 126.1° E) located south of the Yellow Sea.

Although there was no instrument capable of measuring particle size distribution onboard, such information can be inferred from the $N_{CCN}0.6/N_{CN}$ data obtained from the aircraft measurements. During the vertical soundings, layers of low (< 0.3) $N_{CCN}0.6/N_{CN}$ compared to those (~ 0.6) at other altitudes were identified. Small particles generally require high S to activate as CCN. So the significantly lower $N_{CCN}0.6/N_{CN}$ may imply that a greater portion of the particles is too small to activate at the given S of 0.6 %. Such phenomena occurred 16 times during the vertical soundings. Yet one cannot rule out the possibility that such low (< 0.3) $N_{CCN}0.6/N_{CN}$ may be due to the presence of large particles that have low hygroscopicity. Moreover, the fact that there existed small particles alone may not be sufficient for regarding such phenomena as a particle formation and growth event.

So we analyze the aerosol size distribution data measured with an SMPS at KGAWC located at the western coast of the Korean Peninsula. For all three low $N_{CCN}0.6/N_{CN}$ events that took place over the regions I and II below 1000 m altitude, an enhanced nucleation mode is found from the SMPS measurement at KGAWC, confirming that a particle formation and growth event had occurred. Conversely, on the days when low

ACPD
14, 8095–8142, 2014

$N_{CCN}0.6/N_{CN}$ is not observed, a particle formation event is not observed at KGAWC. Such correspondence strongly supports our claim that low $N_{CCN}0.6/N_{CN}$ is a sign of a particle formation and growth event.

The research flight on 18 October 2009 conducted between 12:14 and 15:10 LT along the Yellow Sea route provides a unique opportunity to demonstrate the spatial scale of particle formation and growth event occurred over the Yellow Sea on this day. Low $N_{CCN}0.6/N_{CN}$ at the altitudes below 1000 m is observed in all three spiraling vertical soundings (Fig. 15b) (also during the takeoff and landing). Both SMPS measurements at KGAWC and Gosan (33.2° N, 126.1° E) indicate a particle formation and growth event during the flight duration (Fig. 15c and d, respectively). It was very sunny on this day. The 3 day HYSPLIT back-trajectories at 500 m altitude (Draxler and Rolph, 2013; Rolph, 2013) for the three sounding locations and Tae-An Airport consistently indicate that the air mass is originated from the remote continental region, suggesting that this region is under the influence of an identical air mass (Fig. 16a). The sunny weather condition and the remote continental origin of the air mass for this event is consistent with the finding by Yum et al. (2007) who reported that such condition is favorable for the particle formation and growth events that took place at Gosan, Jeju Island.

The composite of the vertical soundings and the surface measurements at KGAWC and Gosan lead us to suggest that the spatial extent of the particle formation and growth event that took place in the boundary layer on 18 October 2009 covers at least 100 km × 450 km areal extent over the Yellow Sea (Fig. 15a). Considering that the event lasted more than several hours at KGAWC and Gosan, the affected area may have been extended even farther out to the upwind region by several hundred kilometers (Yum et al., 2007; Hussein et al., 2009). This argument is in accordance with Buzorius et al. (2004), Yum et al. (2007) and Kim et al. (2009), where the authors independently suggested that the particle formation and growth event in this region is not a local event but is rather taking place at a regional scale spanning several hundred kilometers across.

ACPD
14, 8095–8142, 2014

In several occasions, low $N_{CCN}0.6/N_{CN}$ is observed at a confined layer above 1000 m altitude, a good example of which is shown in Fig. 17. The 3 day back-trajectories for these occasions also indicated remote continental origin (Fig. 16b). Although we cannot provide direct evidence (e.g., SMPS measurement data) of particle formation and growth event for such layers, it can be suspected that some kind of secondary particle formation event occurred in the free troposphere or at the entrainment layer as previously suggested by McNaughton et al. (2004) and Buzorius et al. (2004) for the Yellow Sea region.

4.2 Composite map of N_{CN} and $N_{CCN}0.6$ near the surface altitudes

Figure 18 provides a composite map of N_{CN} and $N_{CCN}0.6$ near the surface altitudes in and around the Korean Peninsula. Here not only the data analyzed in this study but also the data presented in several previous studies are combined together. Notably the very same instruments were used in all but one (Yum et al., 2005) study. The measurement platforms include ground stations, ship and aircraft, and the total span of the measurement period is 8 years. For the aircraft measurement, only the data below 1000 m altitude were considered. Although each measurement activity was conducted under different meteorological conditions, seasons and years, one can still find some general characteristics of the aerosol distributions over this region.

First, the overall averages of N_{CN} and $N_{CCN}0.6$ range 2500–20 000 cm^{-3} and 1000–5000 cm^{-3}, respectively. According to a study that compiled various studies from around the globe (Andreae, 2009), such level of concentrations corresponds to the condition of polluted marine or continental.

Second, N_{CN} and $N_{CCN}0.6$ over the Yellow Sea and East China Sea, although measured at least 100 km away from the land, are comparable to or even higher than the ones measured at the sites on the islands near by the Korean Peninsula such as Baengyeongdo (J. H. Kim et al., 2011), Yeongjongdo (Kim et al., 2012) or Jeju Island (Yum et al., 2007; J. H. Kim et al., 2011). Moreover, the concentrations observed

ACPD
14, 8095–8142, 2014

at the western part of the Korean Peninsula tend to be higher than the ones measured at the eastern part of the Korean peninsula and over the East Sea, which agrees well with what Y.-J. Kim et al. (2011) found from the satellite retrieval of AOD. This trend indicates that continental outflow is dominantly affecting the aerosol characteristics over the region.

Third, while N_{CN} in Seoul are higher than those at all other locations in this region by about or more than a factor of two, N_{CCN}0.6 in Seoul is not as conspicuously higher and is actually comparable to the ones measured at Anmyeon (Yum et al., 2005) and Baengyeongdo (Kim et al., 2012). Interestingly, N_{CCN}0.6 measured in Tokyo (1760 cm^{-3}, from Kuwata and Kondo, 2008) is quiet comparable to the ones obtained at Daegwallyeong and over the East Sea. It may be suggested that local sources in Seoul contribute dominantly to N_{CN} but not to N_{CCN}0.6, and that the majority of CCN in Seoul has its origin in continental outflow that affects the whole Korean Peninsula. Such explanation is in accordance with the discussion in Sect. 2.2.

5 Summary

Total number concentrations of particles having diameter larger than 10 nm (N_{CN}), cloud condensation nuclei at several supersaturation values (N_{CCN}), and the number size distribution of particles for 10–414 nm particle diameter range were measured in Seoul between 2004 and 2010. The result illustrates that the concentrations are the highest during the winter and the minimum occurs in summer, perhaps largely due to the monsoon circulation. The elevated heating emission locally in Seoul and also in China may have contributed to the highest concentrations in winter, although no conclusive evidence is provided. Traffic emission profoundly influences the diurnal variation of N_{CN} but its influence on N_{CCN} is rather limited. In contrast, there is a strong negative relationship between N_{CCN} and planetary boundary layer (PBL) height (N_{CCN} decreased as PBL expands) but this is not the case for N_{CN}. Such findings suggest

ACPD
14, 8095–8142, 2014

that a significant portion of CCN measured in Seoul may not be directly originated from local sources.

N_{CN} and N_{CCN} at 0.6 % supersaturation were measured during the aircraft measurement campaigns in 2009 and 2011. The vertical structure of N_{CN} and $N_{CCN}0.6$ reveals that the concentrations in the lower altitudes were generally higher than at higher altitudes, except for the cases when particle formation and growth events are thought to occur at higher altitudes. N_{CN} and N_{CCN} show generally a positive correlation with aerosol scattering coefficients measured by a nephelometer but its correspondence tends to vary with altitude. Occasional instances of low (< 0.3) $N_{CCN}0.6/N_{CN}$ in the boundary layer are demonstrated to be associated with particle formation and growth events. With the support of ground measurements, it is confirmed that a particle formation and growth event indeed occurred on a flight day over the Yellow Sea and the areal extent of the event is estimated to be greater than 100 km × 450 km.

The composite map of the aerosol distributions near the surface altitudes in and around the Korean Peninsula is constructed by combining the data analyzed in this study and those presented in several previous measurement studies in this region (Fig. 18). This map is the product of 8 years long effort to measure the aerosol distribution and CCN concentration in this region. Considering the fact that cloud droplet concentrations are directly determined by the CCN concentration at cloud base altitudes and the further growth of the cloud and its radiative properties are in turn highly dependent on cloud droplet concentrations, the data shown in this map is highly expected to be used as a valuable reference dataset for modeling studies that assess the aerosol indirect effects in the East Asian region. Applicability can also be found for the validation of the satellite remote sensing of the aerosol distribution in this region. Overall, the exhibited concentrations are representative of the values measured over the polluted regions elsewhere in the globe. There is also a generally decreasing trend from west to east over the region, implying that the region is constantly under the dominant influence of continental outflow.

ACPD
14, 8095–8142, 2014

Acknowledgements. The authors gratefully acknowledge the NOAA Air Resources Laboratory (ARL) for the provision of the HYSPLIT transport and dispersion model and/or READY website (http://ready.arl.noaa.gov) used in this publication. This work is funded by the Korea Meteorological Administration Research and Development Program under Grant CATER_2012-3051.

References

Adhikari, M., Ishizaka, Y., Minda, H., Kazaoka, R., Jensen, J. B., Gras, G. L., and Nakajima, T.: Vertical distribution of cloud condensation nuclei concentrations and their effect on microphysical properties of clouds over the sea near the southwest islands of Japan, J. Geophys. Res., 110, D10203, doi:10.1029/2004JD004758, 2005.

Andreae, M. O.: Correlation between cloud condensation nuclei concentration and aerosol optical thickness in remote and polluted regions, Atmos. Chem. Phys., 9, 543–556, doi:10.5194/acp-9-543-2009, 2009.

Asmi, A., Wiedensohler, A., Laj, P., Fjaeraa, A.-M., Sellegri, K., Birmili, W., Weingartner, E., Baltensperger, U., Zdimal, V., Zikova, N., Putaud, J.-P., Marinoni, A., Tunved, P., Hansson, H.-C., Fiebig, M., Kivekäs, N., Lihavainen, H., Asmi, E., Ulevicius, V., Aalto, P. P., Swietlicki, E., Kristensson, A., Mihalopoulos, N., Kalivitis, N., Kalapov, I., Kiss, G., de Leeuw, G., Henzing, B., Harrison, R. M., Beddows, D., O'Dowd, C., Jennings, S. G., Flentje, H., Weinhold, K., Meinhardt, F., Ries, L., and Kulmala, M.: Number size distributions and seasonality of submicron particles in Europe 2008–2009, Atmos. Chem. Phys., 11, 5505–5538, doi:10.5194/acp-11-5505-2011, 2011.

Bodhaine, B. A., Ahlquist, N. C., and Schnell, R. C.: Three-wavelength nephelometer suitable for aircraft measurement of background aerosol scattering coefficient, Atmos. Environ., 25, 2267–2276, 1991.

Brooks, I. M.: Find boundary layer top: application of a wavlet covariance transform to lidar backscatter profiles, J. Atmos. Ocean. Tech., 20, 1092–1105, 2003.

Buzorius, G., McNaughton, C. S., Clarke, A. D., Covert, D. S., Blomquist, B., Nielsen, K., and Brechtel, F. J.: Secondary aerosol formation in continental outflow conditions during ACE-Asia, J. Geophys. Res., 109, D24203, doi:10.1029/2004JD004749, 2004.

Clarke, A. and Kapustin, V.: Hemispheric aerosol vertical profiles: anthropogenic impacts on optical depth and cloud nuclei, Science, 329, 1488–1492, 2010.

Crutzen, P.: Albedo enhancement by stratospheric sulfur injections: a contribution to resolve a policy dilemma?, Climatic Change, 77, 211–219, doi:10.1007/s10584-006-9101-y, 2006.
Draxler, R. R. and Rolph, G. D.: HYSPLIT (HYbrid Single-Particle Lagrangian Integrated Trajectory) Model access via NOAA ARL READY Website, available at: http://ready.arl.noaa.gov/HYSPLIT.php (last access: 23 May 2013), NOAA Air Resources Laboratory, Silver Spring, MD, USA, 2013.
Hudson, J. G, Xie, Y., and Yum, S. S.: Vertical distributions of cloud condensation nuclei spectra over the summertime Southern Ocean, J. Geophys. Res., 103, 16609–16624, 1998.
Hussein, T., Junninen, H., Tunved, P., Kristensson, A., Dal Maso, M., Riipinen, I., Aalto, P. P., Hansson, H.-C., Swietlicki, E., and Kulmala, M.: Time span and spatial scale of regional new particle formation events over Finland and Southern Sweden, Atmos. Chem. Phys., 9, 4699–4716, doi:10.5194/acp-9-4699-2009, 2009.
IPCC: Climate Change 2007: The Physical Science Basis, Contribution of Working Group I to the Fourth Assessment Report of the Intergovernmental Panel on Climate Change, edited by: Solomon, S., Qin, D., Manning, M., Chen, Z., Marquis, M., Averyt, K. B., Tignor, M., and Miller, H. L., Cambridge University Press, Cambridge, 1056 pp., 2007.
Kiehl, J. T.: Twentieth century climate model response and climate sensitivity, Geophys. Res. Lett., 34, L22710, doi:10.1029/2007GL031383, 2007.
Kim, J.: Transport routes and source regions of Asian dust observed in Korea during the past 40 years (1965–2004), Atmos. Environ., 42, 4778–4789, 2008.
Kim, J. H., Yum, S. S., Shim, S., Yoon, S.-C., Hudson, J. G., Park, J., and Lee, S.-J.: On aerosol hygroscopicity, cloud condensation nuclei (CCN) spectra and critical supersaturation measured at two remote islands of Korea between 2006 and 2009, Atmos. Chem. Phys., 11, 12627–12645, doi:10.5194/acp-11-12627-2011, 2011.
Kim, J. H., Park, M., Shim, S., and Yum, S. S.: On the contrast of aerosol size distribution and cloud condensation nuclei concentrations between the east and the west of the Korean Peninsula, Atmosphere, 22, 87–96, 2012 (in Korean).
Kim, S.-W., Yoon, S.-C., Won, J.-G., and Choi, S.-C.: Ground-based remote sensing measurements of aerosol and ozone in an urban area: a case study of mixing height evolution and its effect on ground-level ozone concentrations, Atmos. Environ., 41, 7069–7081, 2007.
Kim, Y., Yoon, S.-C., Kim, S.-W., Kim, K.-Y., Lim, H.-C., and Ryu, J.: Observation of new particle formation and growth events in Asian continental outflow, Atmos. Environ., 64, 160–168, 2013.

ACPD
14, 8095–8142, 2014

Kim. Y.-J., Lee, J.-H., and Kim, B.-G.: An analysis of aerosol-cloud relationship using MODIS and NCEP/NCAR reanalysis data around Korea, J. Korean Soc. Atmos. Environ., 27, 152–167, 2011.
Kumala, M., Vehkamaki, H., Petaja, T., Dal Maso, M., Lauri, A., Kerminen, V.-M., Birmili, W., and McMurry, P. H.: Formation and growth rates of ultrafine atmospheric particles: a review of observations, J. Aerosol Sci., 35, 143–176, 2004.
Kuwata, M. and Kondo, Y.: Dependence of size-resolved CCN spectra on the mixing state of nonvolatile cores observed in Tokyo, J. Geophys. Res., 113, D19202, doi:10.1029/2007JD009761, 2008.
Kuwata, M., Kondo, Y., Miyazaki, Y., Komazaki, Y., Kim, J. H., Yum, S. S., Tanimoto, H., and Matsueda, H.: Cloud condensation nuclei activity at Jeju Island, Korea in spring 2005, Atmos. Chem. Phys., 8, 2933–2948, doi:10.5194/acp-8-2933-2008, 2008.
Lee, Y.-G., Lee, H.-W., Kim, M. S., Choi, C. Y., and Kim, J.: Characteristics of particle formation events in the coastal region of Korea in 2005, Atmos. Environ., 42, 3729–3739, 2008.
Matsumoto, K., Tanaka, H., Nagao, I., and Ishizaka, Y.: Contribution of particulate sulfate and organic carbon to cloud condensation nuclei in the marine atmosphere, Geophys. Res. Lett., 24, 665–658, 1997.
McNaughton, C. S., Clarke, A. D., Howell, S. G., Moore II, K. G., Brekhovskikh, V., Weber, R. J., Orsini, D. A., Covert, D. S., Buzorius, G., Brechtel, F. J., Carmichael, G. R., Tang, Y., Eisele, F. L., Mauldin, R. L., Bandy, A. R., Thornton, D. C., and Blomquist, B.: Spatial distribution and size evolution of particles in Asian outflow: significance of primary and secondary aerosols during ACE-Asia and TRACE-P, J. Geophys. Res., 109, D19S06, doi:10.1029/2003JD003528, 2004.
Mochida, M., Nishita-Hara, C., Kitamori, Y., Aggarwal, S. G., Kawamura, K., Miura, K., and Takami, A.: Size-segregated measurements of cloud condensation nucleus activity and hygroscopic growth for aerosols at Cape Hedo, Japan, in spring 2008, J. Geophys. Res., 115, D21207, doi:10.1029/2009JD013216, 2010.
Mönkkönen, P., Koponen, I. K., Lehtinen, K. E. J., Hämeri, K., Uma, R., and Kulmala, M.: Measurements in a highly polluted Asian mega city: observations of aerosol number size distribution, modal parameters and nucleation events, Atmos. Chem. Phys., 5, 57–66, doi:10.5194/acp-5-57-2005, 2005.

ACPD
14, 8095–8142, 2014

On the submicron aerosol distributions and CCN number concentrations

J. H. Kim et al.

Pandey, S. K., Kim, K.-H., Chung, S.-Y., Cho, S.-J., Kim, M.-Y., and Sho, Z.-H.: Long-term study of NO_x behavior at urban roadside and background locations in Seoul, Korea, Atmos. Environ., 42, 607–622, 2008.
Park, K., Park., J. Y., Kwak, J.-H., Cho, G. N., and Kim, J.-S.: Seasonal and diurnal variations of ultrafine particle concentration in urban Gwangju, Korea: observation of ultrafine particle events, Atmos. Environ., 42, 788–799, 2008.
Roberts, G. C. and Nenes, A.: A continuous-flow streamwise thermal-gradient CCN chamber for atmospheric measurements, Aerosol Sci. Tech., 39, 206–221, 2005.
Robock, A.: 20 reasons why geoengineering may be a bad idea, B. Atom. Sci., 64, 14–18, 2008.
Rogelj, J., Hare, W., Lowe, J., van Vuuren, D. P., Riahi, K., Matthews, B., Hanaoka, T., Jiang, K., and Meinshausen, M.: Emission pathways consistent with a 2 °C global temperature limit, Nature Climate Change, 1, 413–418, 2011.
Rolph, G. D.: Real-time Environmental Applications and Display sYstem (READY) Website, available at: http://ready.arl.noaa.gov (last access: 23 May 2013), NOAA Air Resources Laboratory, Silver Spring, MD, 2013.
Rose, D., Nowak, A., Achtert, P., Wiedensohler, A., Hu, M., Shao, M., Zhang, Y., Andreae, M. O., and Pöschl, U.: Cloud condensation nuclei in polluted air and biomass burning smoke near the mega-city Guangzhou, China – Part 1: Size-resolved measurements and implications for the modeling of aerosol particle hygroscopicity and CCN activity, Atmos. Chem. Phys., 10, 3365–3383, doi:10.5194/acp-10-3365-2010, 2010.
Schwartz, S. E., Charlson, R. J., Khan, R. A., Ogren, J. A., and Rodhe, H.: Why hasn't Earth warmed as much as expected?, J. Climate, 23, 2453–2464, 2010.
Shim, S., Yoon, Y. J., Yum, S. S., Cha, J. W., Kim, J. H., Kim, J., and Lee., B.-Y.: Nephelometer measurement of aerosol scattering coefficient at Seoul, Atmosphere, 18, 459–474, 2008 (in Korean).
Song, M., Lee, M., Kim, J. H., Yum, S. S., Lee, G., and Kim, K.-R.: New particle formation and growth in relation to vertical mixing and chemical species during ABC-EAREX2005, Atmos. Res., 97, 359–370, 2010.
Weber, R. J., Lee, S., Chen, G., Wang, B., Kapustin, V., Moore, K., Clarke, A. D., Mauldin, L., Kosciuch, E., Cantrell, C., Eisele, F., Thornton, D. C., Bandy, A. R., Sachse, G. W., and Fuelberg, H. E.: New particle formation in anthropogenic plumes advecting from Asia observed during TRACE-P, J. Geophys. Res., 108, 8814, doi:10.1029/2002JD003112, 2003.

ACPD
14, 8095–8142, 2014

On the submicron aerosol distributions and CCN number concentrations

J. H. Kim et al.

Wiedensohler, A., Cheng, Y. F., Nowak, A., Wehner, B., Achtert, P., Berghof, M., Birmili, W., Wu, Z. J., Hu, M., Zhu, T., Takegawa, N., Kita, K., Kondo, Y., Lou, S. R., Hofzumahaus, A., Holland, F., Wahner, A., Gunthe, S. S. Rose, D., Su, H., and Pöschl, U.: Rapid aerosol particle growth and increase of cloud condensation nucleus activity by secondary aerosol formation and condensation: a case study for regional air pollution in northeastern China, J. Geophys. Res., 114, D00G08, doi:10.1029/2008JD010884, 2009.

Wu, Z., Hu, M., Liu, S., Wehner, B., Bauer, S., Maßling, A., Wiedensohler, A., Petäjä, T., Maso, M. D., and Kulmala, M.: New particle formation in Beijing, China: statistical analysis of a 1-year data set, J. Geophys. Res., 112, D09209, doi:10.1029/2006JD007406, 2007.

Yum, S. S., Hudson, J. G., Song, K. Y., and Choi, B.-C.: Springtime cloud condensation nuclei concentrations on the west coast of Korea, Geophys. Res. Lett., 32, L09814, doi:10.1029/2005GL022641, 2005.

Yum, S. S., Roberts, G., Kim, J. H., Song, K., and Kim, D.: Submicron aerosol size distributions and cloud condensation nuclei concentrations measured at Gosan, Korea, during the Atmospheric Brown Clouds-East Asian Regional Experiment 2005, J. Geophys. Res., 112, D22S32, doi:10.1029/2006JD008212, 2007.

Zhang, Z. Q. and Liu, B. Y. H.: Performance of TSI 3760 CNC at reduced pressures and flow rates, Aerosol Sci. Tech., 15, 228–238, 1991.

ACPD
14, 8095–8142, 2014

Table 1. List of the vertical soundings obtained during the 2009 and 2011 campaigns.

Vertical soundings	Date	Beginning time (LT)	End time (LT)	Location (° N, ° E)	Region	Data count[b]	Data count[c]
1	5 Oct 2009	14:35:54	14:43:59	33.41, 125.81	Western coast	142	
2	6 Oct 2009[a]	10:23:53	10:28:15	33.40, 125.79	Western coast	89	
3	6 Oct 2009[a]	14:55:48	15:07:11	33.47, 126.41	Western coast	170	
4	6 Oct 2009[a]	16:39:30	16:45:27	33.42, 124.70	Yellow Sea	99	
5	6 Oct 2009[a]	17:42:04	17:46:44	36.56, 124.72	Yellow Sea	95	
6	10 Oct 2009	14:32:15	14:37:47	36.71, 131.17	East Sea	333	
7	10 Oct 2009	14:52:54	14:56:21	37.46, 131.14	East Sea	208	
8	11 Oct 2009	14:37:31	14:43:27	36.71, 131.14	East Sea	357	
9	11 Oct 2009	14:57:51	15:04:35	37.50, 131.13	East Sea	349	
10	12 Oct 2009	09:53:13	09:58:58	36.72, 131.15	East Sea	346	
11	12 Oct 2009	10:11:00	10:21:08	37.38, 131.20	East Sea	302	
12	12 Oct 2009	11:29:46	11:38:50	37.58, 126.70	Western coast	517	
13	15 Oct 2009	10:18:22	10:24:25	36.74, 131.13	East Sea	364	
14	15 Oct 2009	10:36:26	10:44:58	37.47, 131.19	East Sea	513	
15	18 Oct 2009	12:40:16	12:48:43	36.58, 124.79	Western coast	379	
16	18 Oct 2009	13:37:38	13:48:06	33.47, 124.73	Yellow Sea	587	
17	18 Oct 2009	14:00:00	14:09:42	33.40, 125.81	Yellow Sea	531	
1	8 Jun 2011	14:17:39	14:26:58	34.97, 124.73	Yellow Sea	512	477
2	8 Jun 2011	14:55:14	15:05:04	33.50, 124.83	Yellow Sea	539	354
3	8 Jun 2011	15:18:22	15:28:13	33.50, 125.70	Western coast	541	423
4	11 Jun 2011	12:21:12	12:31:42	37.34, 130.97	East Sea	588	262
5	11 Jun 2011	12:46:35	12:56:20	36.78, 131.01	East Sea	532	219
6	11 Jun 2011	15:43:01	15:52:39	36.39, 126.39	Western coast	541	240
7	12 Jun 2011	10:21:11	10:31:19	37.32, 131.00	East Sea	538	249
8	12 Jun 2011	10:46:17	10:55:57	36.78, 131.03	East Sea	509	146
9	12 Jun 2011	13:43:09	13:54:06	35.75, 124.76	Yellow Sea	576	216
10	12 Jun 2011	14:11:24	14:21:01	36.38, 124.88	Yellow Sea	491	195
11	12 Jun 2011	14:47:53	14:57:51	36.41, 126.39	Western coast	521	106

[a] Two research flights were conducted on 6 October 2009 – one in the morning and another in the afternoon.
[b] For N_{CN}, $N_{CCN}0.6$ and $N_{CCN}0.6/N_{CN}$.
[c] For σ_{450}, σ_{550}, σ_{700}.

ACPD
14, 8095–8142, 2014

On the submicron aerosol distributions and CCN number concentrations

J. H. Kim et al.

Table 2. Average $N_{CCN}0.6$, N_{CN}, $N_{CCN}0.6/N_{CN}$ and the number of data count obtained during the horizontal cruises in each flight of the 2009 and 2011 campaigns.

Year	Date	$N_{CCN}0.6$ (cm^{-3})	N_{CN} (cm^{-3})	$N_{CCN}0.6/N_{CN}$	Data counts
2009	5 Oct	469 ± 95	876 ± 376	0.61 ± 0.17	206
	6 Oct morning	515 ± 130	791 ± 280	0.68 ± 0.17	231
	6 Oct afternoon	494 ± 148	647 ± 198	0.77 ± 0.10	371
	10 Oct	1207 ± 506	1392 ± 504	0.85 ± 0.12	1240
	11 Oct	459 ± 171	632 ± 287	0.74 ± 0.13	3164
	12 Oct	397 ± 144	648 ± 768	0.69 ± 0.15	2477
	15 Oct	641 ± 918	1186 ± 1450	0.55 ± 0.14	2612
	18 Oct	292 ± 119	517 ± 121	0.58 ± 0.21	1819
	2009 Average	559 ± 280	835 ± 304	0.68 ± 0.10	
2011	8 Jun	441 ± 164	851 ± 249	0.51 ± 0.06	1219
	11 Jun	2304 ± 864	3886 ± 1078	0.59 ± 0.10	5856
	12 Jun	2817 ± 1252	3975 ± 1611	0.70 ± 0.05	9178
	2011 Average	1854 ± 1250	2904 ± 1779	0.60 ± 0.09	

ACPD
14, 8095–8142, 2014

Table 3. Average scattering coefficients (σ) at 450, 550 and 700 nm wavelengths, Angström exponent (AE) and the number of data count obtained during the horizontal cruises in each flight of the 2011 campaign.

Year	Date	σ_{450} (Mm^{-1})	σ_{550} (Mm^{-1})	σ_{70} (Mm^{-1})	AE	Data count
2011	8 Jun	18.0 ± 44.3	14.2 ± 34.1	10.1 ± 22.6	1.17 ± 0.90	619
	11 Jun	86.5 ± 36.9	63.3 ± 27.5	40.1 ± 17.8	1.75 ± 0.22	3732
	12 Jun	140.0 ± 65.4	105.5 ± 53.1	70.7 ± 40.4	1.61 ± 0.24	4951

ACPD
14, 8095–8142, 2014

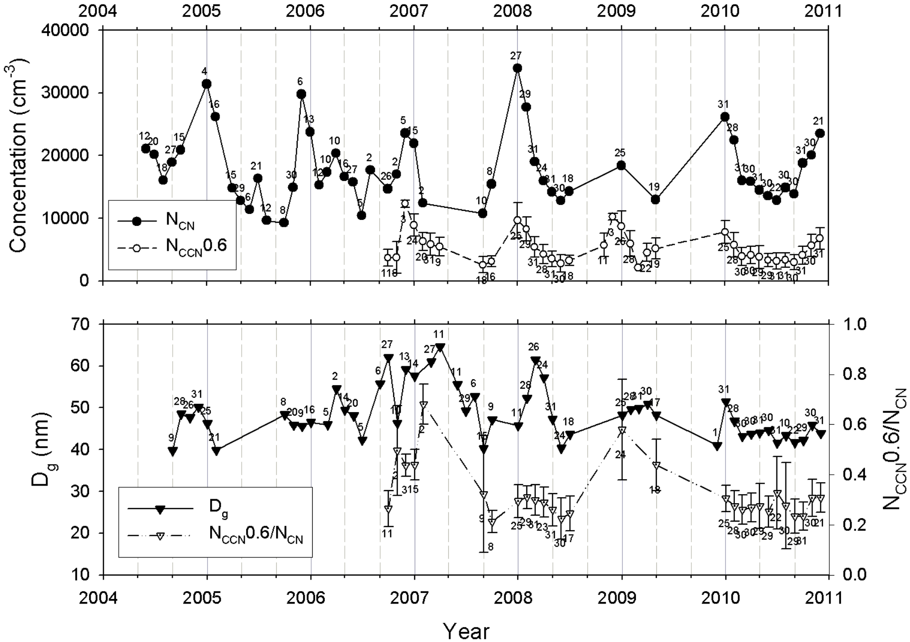

Fig. 1. Time variation of the monthly average values of (top) N_{CN} and $N_{CCN}0.6$, (bottom) D_g and $N_{CCN}0.6/N_{CN}$ meaured in Seoul. The numbers near each symbol indicates the number of measurement days for the month. Error bars for $N_{CCN}0.6$ and $N_{CCN}0.6/N_{CN}$ indicate the standard deviation.

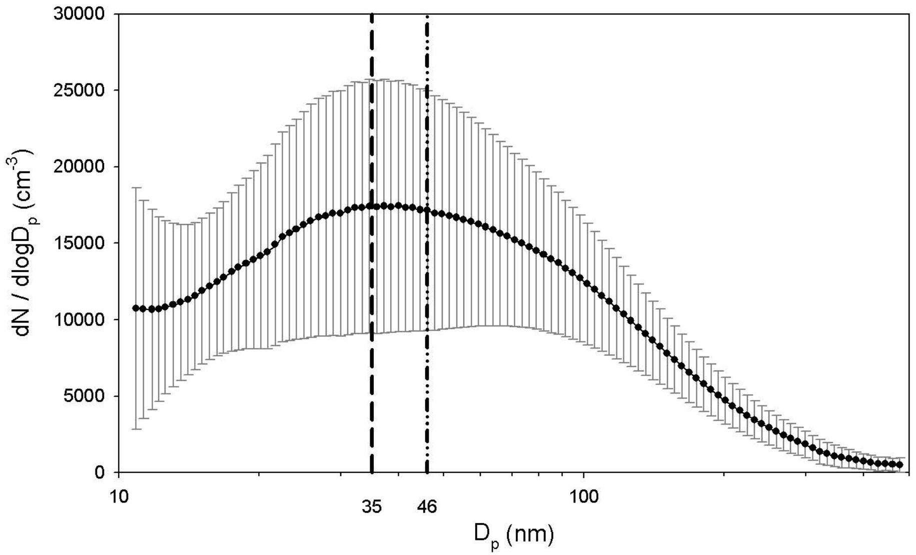

Fig. 2. Overall average aerosol size distribution in Seoul. The error bars indicate the standard deviation value for each size bin. 35 nm (vertical dash line) and 46 nm (vertical dash-dot-dot line) are the mode diameter and geometric mean diameter of the distribution, respectively.

ACPD
14, 8095–8142, 2014

On the submicron aerosol distributions and CCN number concentrations

J. H. Kim et al.

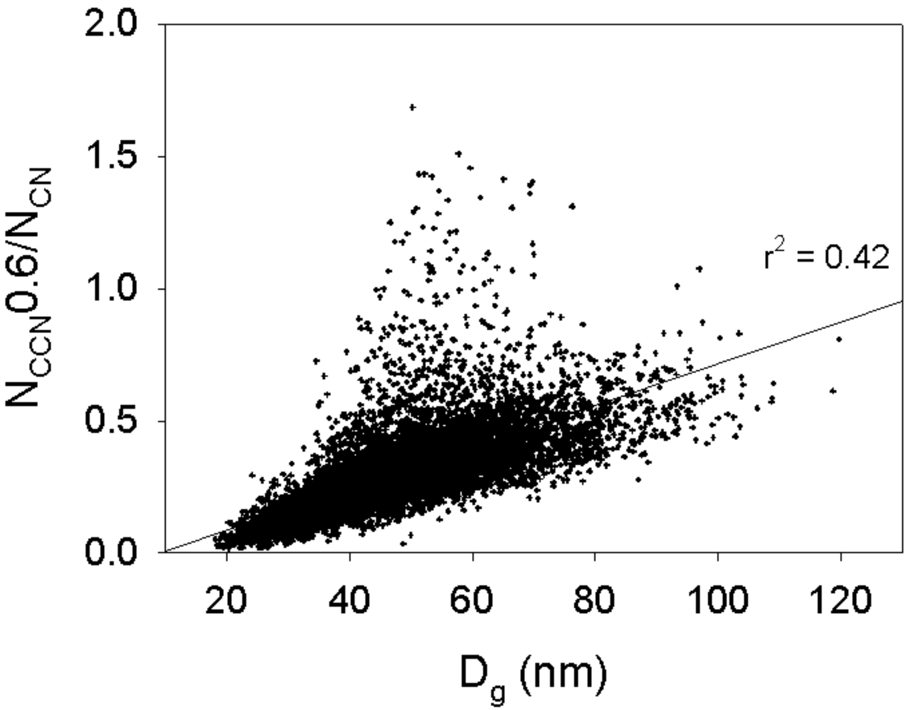

Fig. 3. Scatterplot of D_g vs. $N_{CCN}0.6/N_{CN}$ for hourly averaged data in Seoul. Occasionally the ratio exceeds one due to instrumental differences between TSI CPC 3010 and DMT CCNC. Total number of data was 11 339.

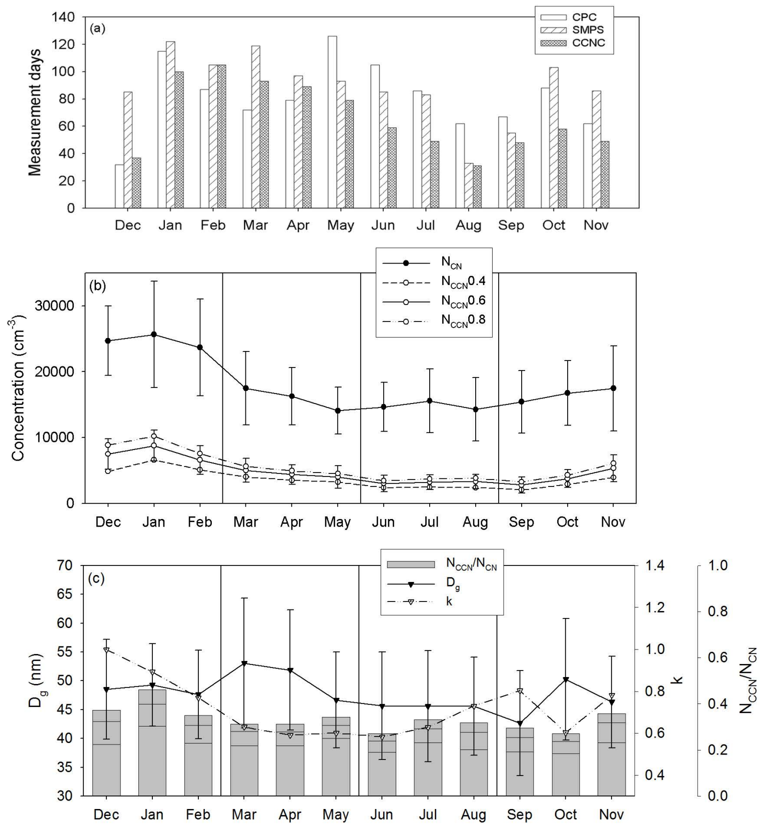

Fig. 4. (a) Distribution of measurement days in Seoul for each month of the years between 2004 and 2010, seasonal variations of **(b)** N_{CN} and N_{CCN}, and **(c)** $N_{\mathrm{CCN}}/N_{\mathrm{CN}}$, D_{g} and parameter k of the Twomey equation ($N = C \times S^k$) in Seoul. In **(b)** and **(c)**, the error bars indicate standard deviation for N_{CN}, $N_{\mathrm{CCN}}0.6$ and D_{g}. In **(c)**, the top, middle and bottom lines within each grey box indicate $N_{\mathrm{CCN}}/N_{\mathrm{CN}}$ for 0.4, 0.6 and 0.8 % S.

ACPD
14, 8095–8142, 2014

On the submicron aerosol distributions and CCN number concentrations

J. H. Kim et al.

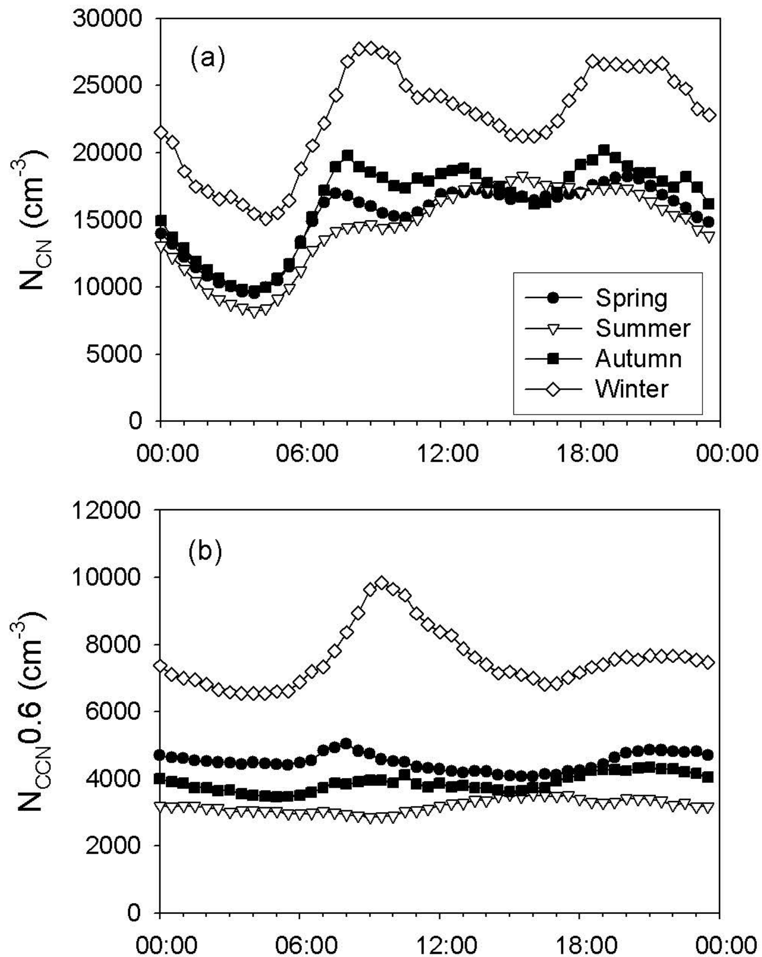

Fig. 5. Average diurnal variation of **(a)** N_{CN} and **(b)** $N_{CCN}0.6$ in Seoul for each season.

ACPD
14, 8095–8142, 2014

On the submicron aerosol distributions and CCN number concentrations

J. H. Kim et al.

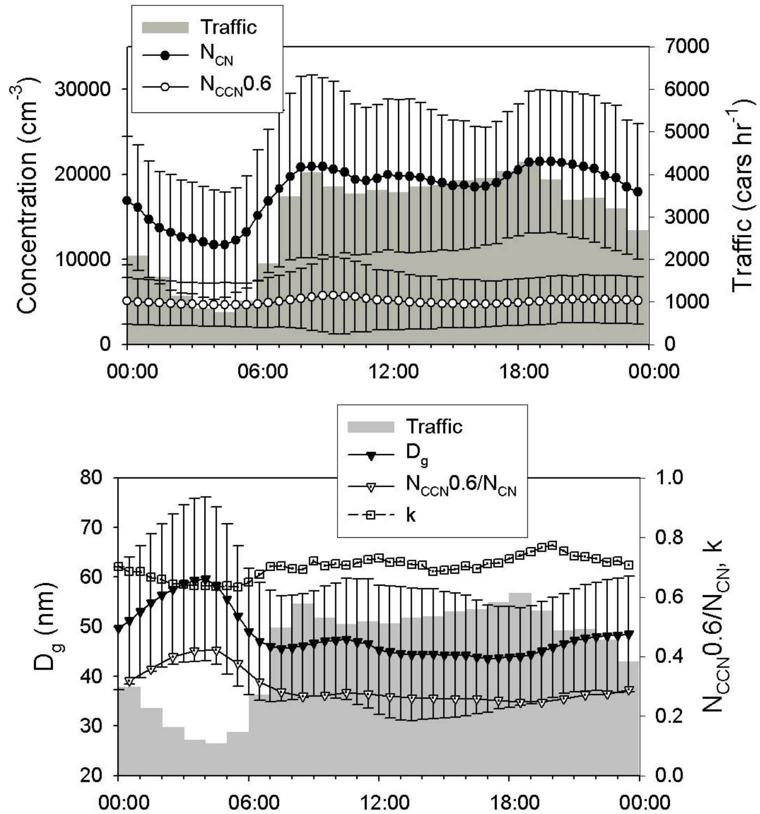

Fig. 6. Average diurnal variation of (top) N_{CN}, $N_{CCN}0.6$ and traffic amount at the nearest major road and (bottom) D_g, $N_{CCN}0.6/N_{CN}$ and k in Seoul. Traffic amount is re-plotted with the same vertical scale at the bottom panel. Error bars indicate standard deviation.

ACPD
14, 8095–8142, 2014

On the submicron aerosol distributions and CCN number concentrations

J. H. Kim et al.

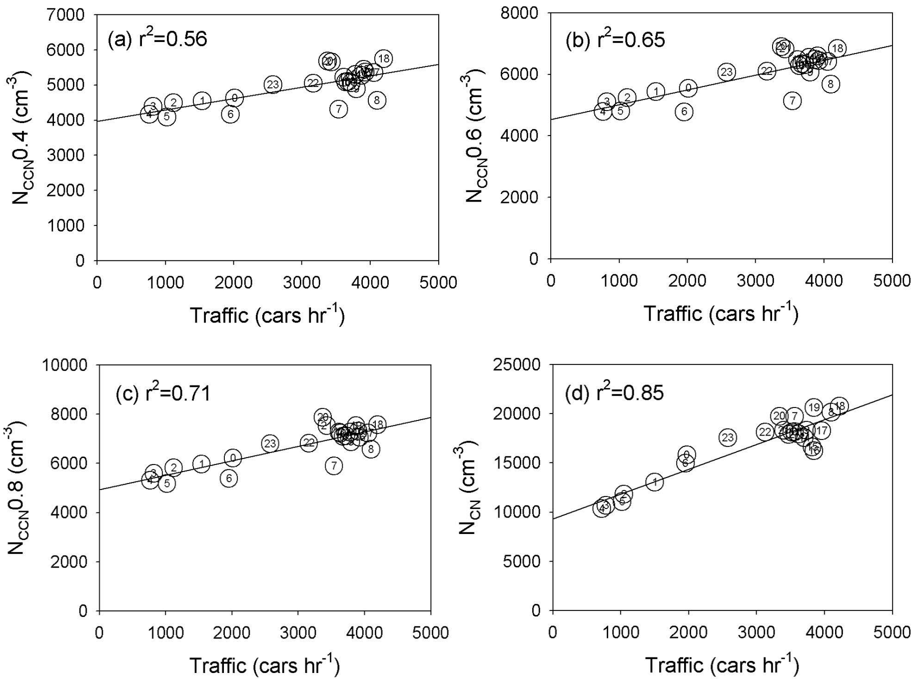

Fig. 7. Scatterplot of traffic amount vs. N_{CCN} at **(a)** 0.4 % S, **(b)** 0.6 % S and **(c)** 0.8 % S, and **(d)** N_{CN} in Seoul. The numbers inside the symbols indicate the hour of the day.

ACPD
14, 8095–8142, 2014

On the submicron aerosol distributions and CCN number concentrations

J. H. Kim et al.

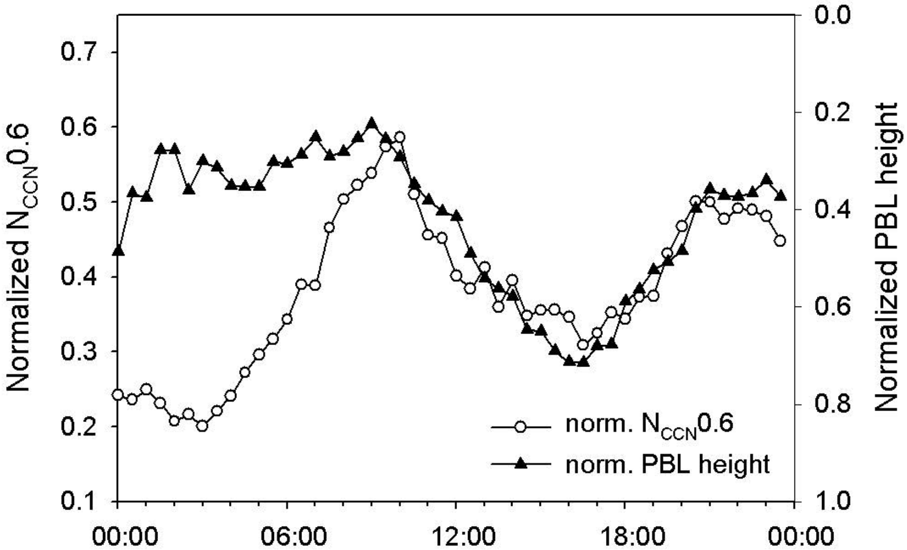

Fig. 8. Average diurnal variation of normalized $N_{CCN}0.6$ and normalized PBL height calculated from MPL data measured on clear days in Seoul. Both vertical axes are scaled to illustrate the diurnal variation and axis for normalized PBL height is reversed for illustration.

ACPD
14, 8095–8142, 2014

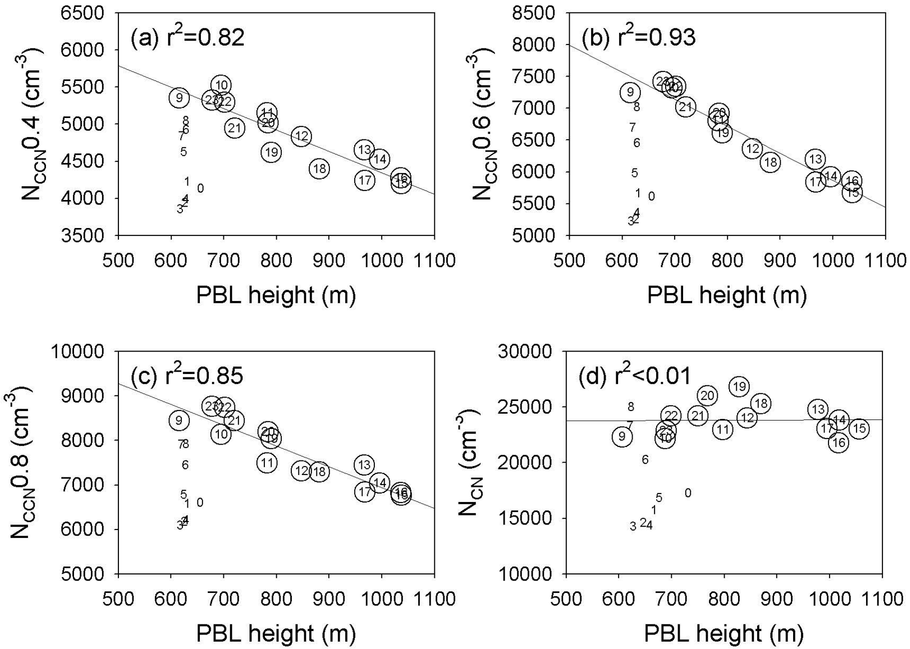

Fig. 9. Scatterplot of PBL height vs. N_{CCN} at **(a)** 0.4 % S, **(b)** 0.6 % S and **(c)** 0.8 % S, and **(d)** N_{CN} in Seoul. The numbers are the hour of the day and the hours between 9 a.m. and midnight are circled to illustrate the relationship. The linear regression line and the coefficient of determination are calculated only for these hours.

ACPD
14, 8095–8142, 2014

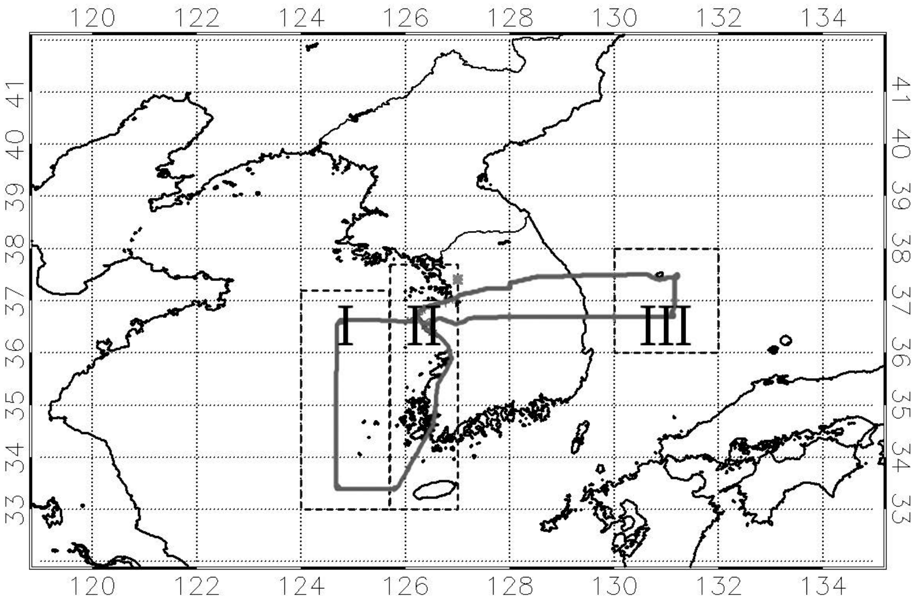

Fig. 10. Classification of regions where vertical measurements were taken place during the 2009 and 2011 campaigns. I: the Yellow Sea, II: west coast of the Korean Peninsula, and III: the East Sea. Two grey loops represent the Yellow Sea route (lies over I and II) and the East Sea route (II and III). The grey square near the upper right corner of region II designates the location of Seoul.

ACPD
14, 8095–8142, 2014

On the submicron aerosol distributions and CCN number concentrations

J. H. Kim et al.

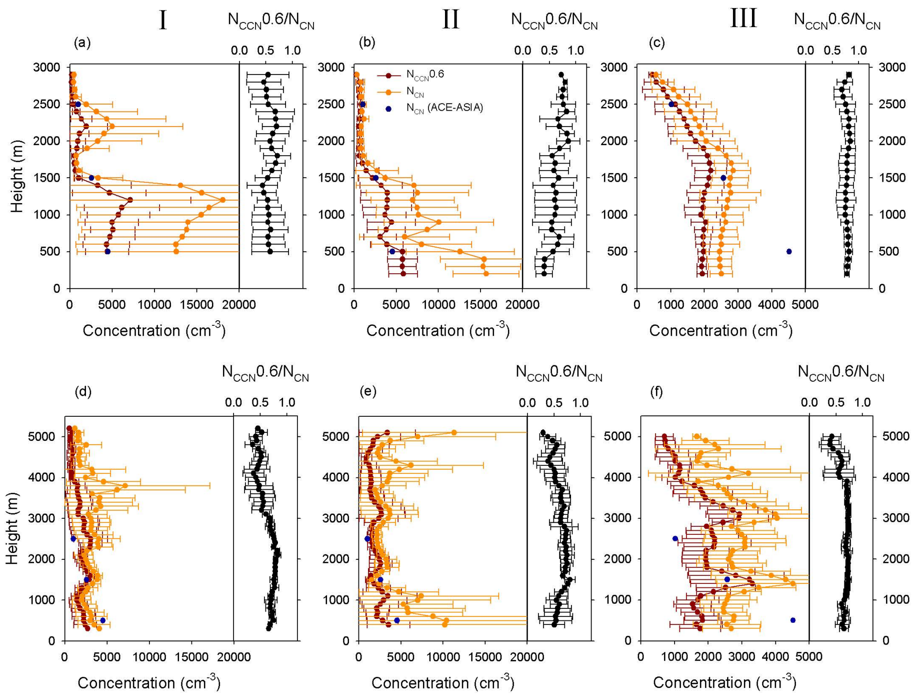

Fig. 11. Average vertical distributions of $N_{CCN}0.6$ (brown), N_{CN} (orange) and $N_{CCN}0.6/N_{CN}$ (black) during the 2009 **(a–c)** and 2011 **(d–f)** campaigns, for each classified region (I, II and III). The averages are taken for each 100 m height bin. Note that the scale of *y* axis is different for the two campaigns. N_{CN} measured during ACE-ASIA (Clarke and Kapustin, 2010) are marked with blue dots for comparison. Error bars denote standard deviations.

ACPD
14, 8095–8142, 2014

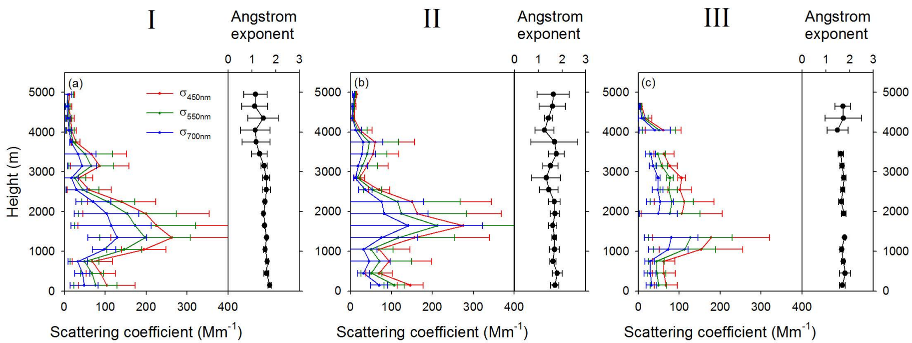

Fig. 12. Average vertical distributions of aerosol scattering coefficient (σ) at 450 (blue), 550 (green) and 700 (red) nm wavelengths during the 2011 campaign for the regions **(a)** I, **(b)** II and **(c)** III, respectively. Corresponding distributions of angstrom exponent are also shown in each panel.

ACPD
14, 8095–8142, 2014

On the submicron aerosol distributions and CCN number concentrations

J. H. Kim et al.

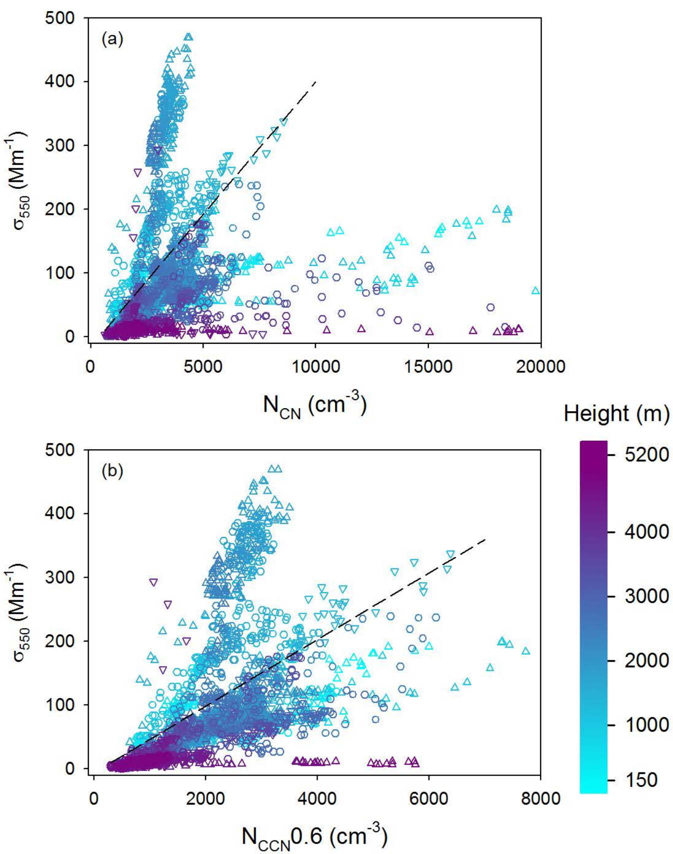

Fig. 13. Scatterplot of simultaneously measured **(a)** N_{CN} vs. σ_{550}, and **(b)** $N_{CCN}0.6$ vs. σ_{550}. The measurement regions I, II and III are denoted by circle, triangle and reverse triangle, respectively. The color of each data represents the altitude of measurement. The dash line is drawn for explanatory purposes for each panel (see text).

ACPD
14, 8095–8142, 2014

On the submicron aerosol distributions and CCN number concentrations

J. H. Kim et al.

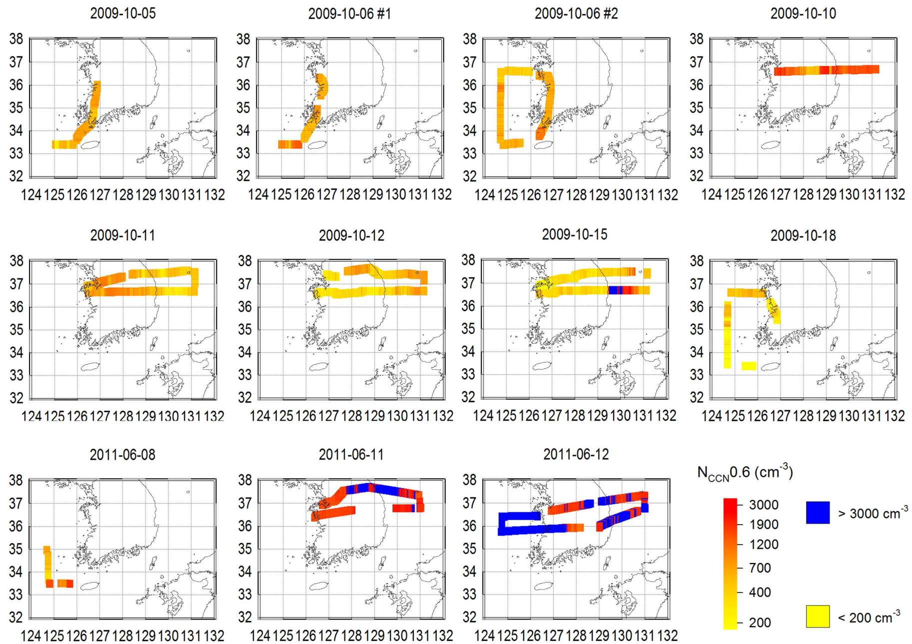

Fig. 14. Horizontal distributions of $N_{CCN}0.6$ for all flights. $N_{CCN}0.6$ below 200 cm^{-3} and above 3000 cm^{-3} are denoted by yellow and blue, respectively. $N_{CCN}0.6$ in between are denoted by the transient color from yellow to red as shown at the bottom right.

ACPD
14, 8095–8142, 2014

On the submicron aerosol distributions and CCN number concentrations

J. H. Kim et al.

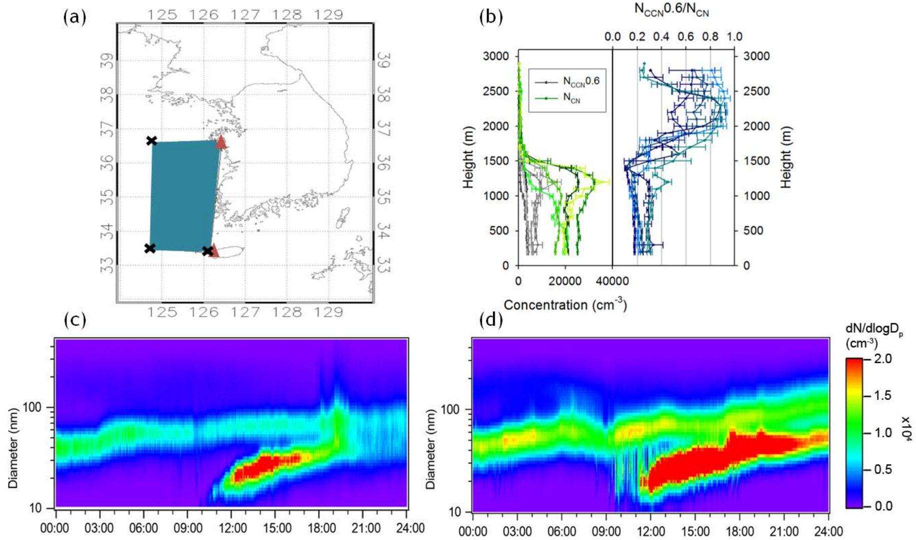

Fig. 15. (a) Locations (X) where low $N_{CCN}0.6/N_{CN}$ is found in the boundary layer during a flight between 12:14 and 15:30 LT on 18 October 2009 and the locations (triangle) of the surface SMPS measurements at KGAWC and Gosan, **(b)** vertical distributions of N_{CN} (green variant), $N_{CCN}0.6$ (gray variant) and $N_{CCN}0.6/N_{CN}$ (blue variant) during this flight, and the time variation of aerosol size distributions measured at **(c)** KGAWC and **(d)** Gosan.

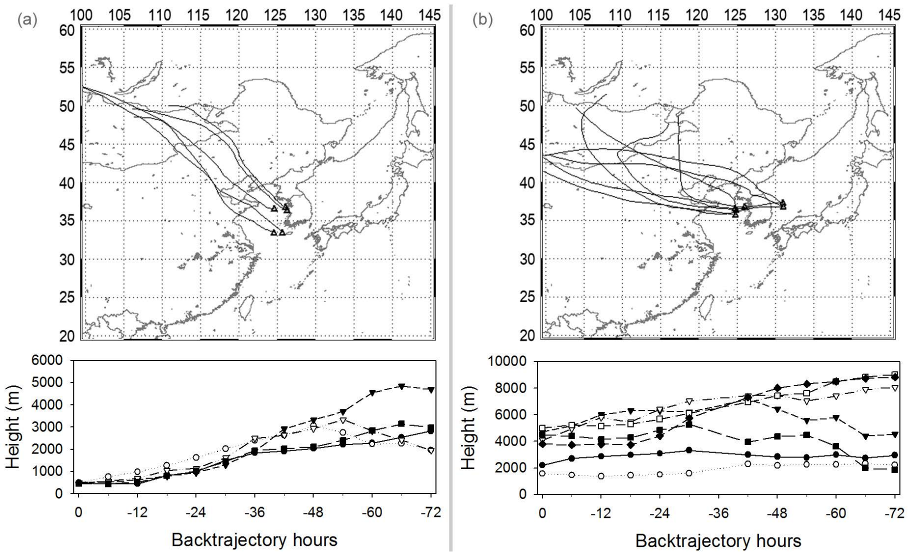

Fig. 16. The 3 day back-trajectories of the air mass at the locations of low $N_{CCN}0.6/N_{CN}$ vertical soundings (left) during the flight on 18 October 2009 and (right) on some other days.

ACPD
14, 8095–8142, 2014

On the submicron aerosol distributions and CCN number concentrations

J. H. Kim et al.

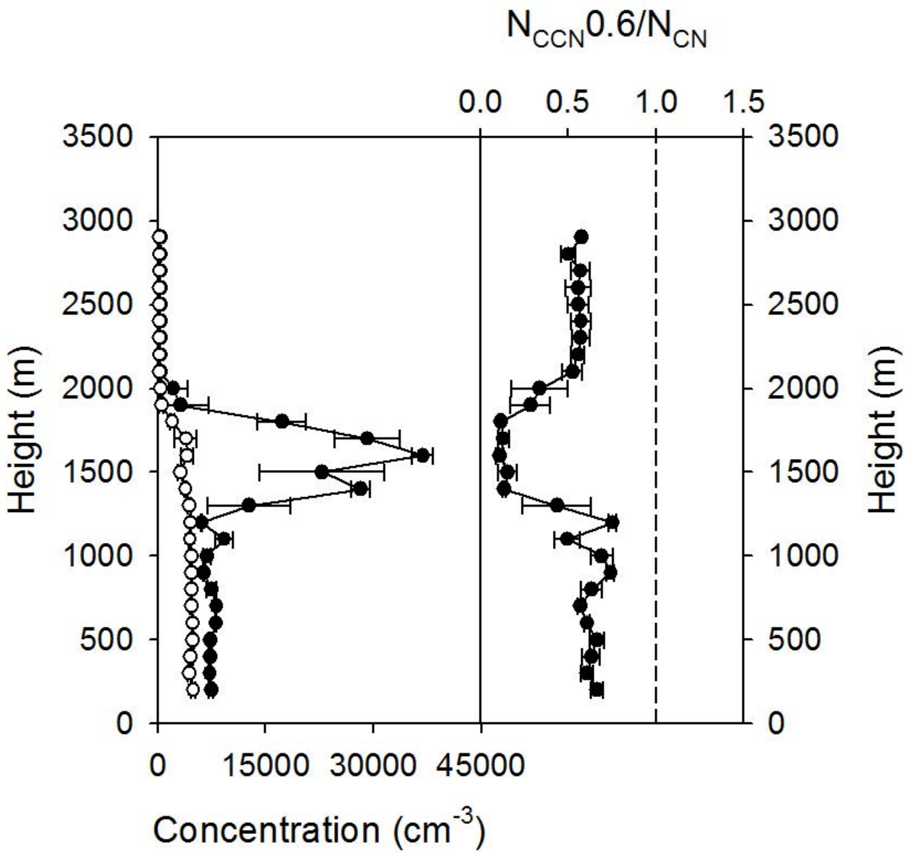

Fig. 17. A typical example of low $N_{CCN}0.6/N_{CN}$ layer aloft (> 1000 m) (on 15 October 2009).

ACPD
14, 8095–8142, 2014

On the submicron aerosol distributions and CCN number concentrations

J. H. Kim et al.

Title Page
Abstract Introduction
Conclusions References
Tables Figures
◀I ▶I
◀ ▶
Back Close
Full Screen / Esc
Printer-friendly Version
Interactive Discussion

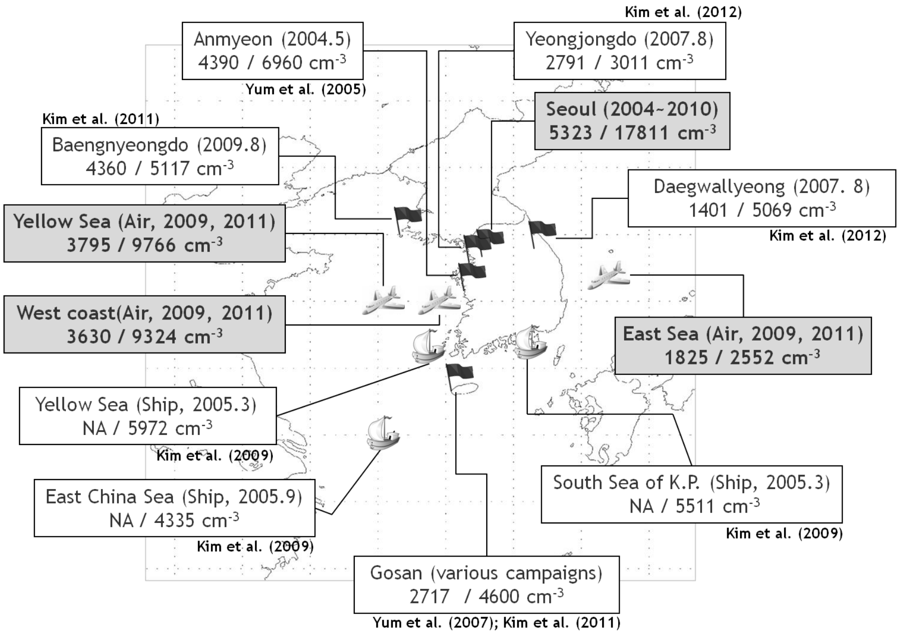

Fig. 18. Composite map of the average $N_{CCN}0.6$ and N_{CN} measured on the ground (flag), over the sea (ship) surface or in the boundary layer below 1100 m altitude (airplane), in and around the Korean Peninsula. The data presented in this study are shown in shaded box.

ACPD
14, 8095–8142, 2014